Enhanced Stability by Three-Dimensional Aromaticity of Endohedrally Doped Clusters X10M0/− with X = Ge, Sn, Pb and M = Cu, Ag, Au

2 AUTHORS:

Truong Tai
University of Leuven
65 PUBLICATIONS **506** CITATIONS

SEE PROFILE

Minh Tho Nguyen
University of Leuven
748 PUBLICATIONS **10,846** CITATIONS

SEE PROFILE

Enhanced Stability by Three-Dimensional Aromaticity of Endohedrally Doped Clusters $X_{10}M^{0/-}$ with X = Ge, Sn, Pb and M = Cu, Ag, Au

Truong Ba Tai[†] and Minh Tho Nguyen[†,‡,*]

[†]Department of Chemistry, Katholieke Universiteit Leuven, B-3001 Leuven, Belgium
[‡]Institute for Computational Science and Technology of HoChiMinhCity, Thu Duc, HoChiMinh City, Vietnam

Ⓢ Supporting Information

ABSTRACT: The group 14 clusters encapsulated by coinage metals in neutral and anionic states $X_{10}M^{0/-}$ (X = Ge, Sn, Pb and M = Cu, Ag, Au) are investigated using quantum chemical calculations with the DFT/B3LYP functional and coupled-cluster CCSD(T) theory. Addition of transition metals into the empty cages forms high symmetry endohedral structures, except for $Ge_{10}Ag^{0/-}$. In agreement with experiments available for $X_{10}Cu$, the D_{4d} global minima of the anions are calculated to be magic clusters with large frontier orbital gaps, high vertical and adiabatic detachment energies, and large embedding energies and binding energies as compared to those of the empty cages X_{10}^{2-}. The enhanced stability of these magic clusters can be rationalized by the three-dimensional aromaticity.

■ INTRODUCTION

The group IVA clusters encapsulated by transition metals continue to attract much attention of scientists in part due to their potential as candidates for designing assembled nanomaterials, and also to their high stability, symmetrical shape, and chemical bonding. A number of experimental and theoretical investigations were performed on the mixed clusters $M@X_n$ with M = metal and X = Si, Ge, Sn, and Pb, not only to gain more insight into their bonding nature and spectroscopic properties but also to obtain the fundamentals for designing new materials.[1−11] Recently, from experimental mass spectrometric results and DFT calculations on mixed cationic clusters AlX_n^+ (X = Si, Ge, Sn, Sn), Lievens and co-workers[12] proposed a general principle for designing highly symmetrical stable clusters that is based on both the three-dimensional aromatic stability and close-packing structures. While metal dopants tend to be encapsulated into empty cages of the heavier elements (Ge, Sn, and Pb), small metal doped silicon clusters usually prefer exohedral structures due to the rather limited size of the empty silicon cages. Additionally, the relative size between the metal dopant M and the empty cages X_n is also one of the important factors that determine the stability and structural features of the mixed clusters $M@X_n$. This effect is even more important for the $M@X_{10}$ clusters in which the ten-atom X_{10} cages are of medium size. For instance, while all transition metal encapsulated clusters $M@X_{10}$ (M = Ni, Pd, Pt, and X = Sn, Pb) possess the bicapped square antiprism structures (D_{4d}), in which the metal M is located at the center of X_{10} cage, the mixed clusters $X_{10}Pt$, with X = Si and Ge, prefer opened structures. The Pd dopant is located outside of

the Si_{10} cage.[13] A similar observation was found for $Pb_{10}M$, M = Mg, Ba, and Sr, where Mg can be encapsulated inside the Pb_{10} cage, whereas the Ba and Sr atoms cap the Pb_{10} block from outside.[14]

While some experimental studies on the doped silicon[15] and germanium[16] clusters were reported, experimental results on the mixed clusters based on the heavier elements of the group IVA are rather limited. Lievens et al.[17] carried out a mass spectrometric stability investigation of a series of metal doped group IVA clusters MX_n, including X = Si, Ge, Sn, Pb and M = Cr, Mn, Cu, Zn. Their experimental results showed that the copper−group IVA element mixed clusters X_nCu (X = Ge, Sn, Pb) exhibit remarkably high abundance at the size n = 10. As a consequence, the corresponding systems such as $CuGe_{10}^+$, $CuSn_{10}^{0,+}$, and $CuPb_{10}^{0,+}$ were established to be the species with enhanced stability. Nevertheless, the reasons for such a phenomenon have not been well understood. It is remarkable to note that theoretical studies on coinage metal group IVA mixed clusters are even more limited. Only a few studies on the Cu and Au doped Ge clusters were recently reported. While $Ge_{10}Cu$ is found to be an endohedral structure (D_{4d}),[18] the isovalent $Ge_{10}Au$ is a C_{2v}-pentagonal prism structure.[19] A legitimate question thus arises about how the coinage metals M (M = Cu, Ag, Au) are located in the empty X_{10} cages with X = Sn and Pb that have larger sizes as compared to the Ge_{10} cage. Additionally, an understanding on their anionic clusters which are very interesting for experimental studies also remains missing.
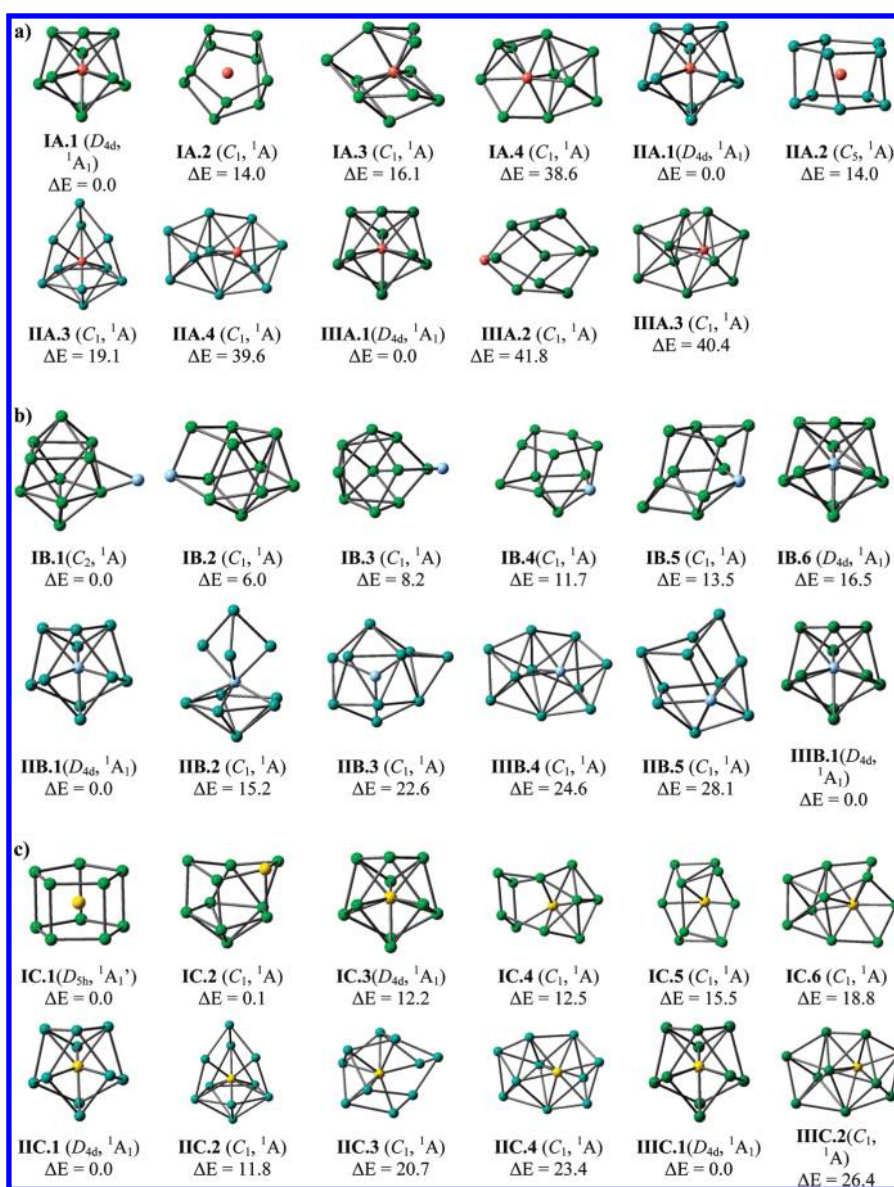
Figure 1. Shapes, point groups, and relative energies (kcal/mol) of some low-lying isomers of the anionic clusters $X_{10}M^-$ (X = Ge, Sn, Pb and M = Cu, Ag, Au) (B3LYP/LanL2DZ): (a) $X_{10}Cu^-$; (b) $X_{10}Ag^-$; (c) $X_{10}Au^-$.

Motivated by these reasons, we set out to carry out a systematic investigation on the clusters with impurity $X_{10}M^{0/-}$ in both neutral and anionic states, in which X = Ge, Sn, Pb and M = Cu, Ag, Au. The location of the lower-lying isomers of the clusters considered is carried out using a stochastic search method.[20] As experimental studies on silver- or gold-doped group 14 clusters are not available, predictions of their properties and additional confirmation on the effects of impurities on the caged clusters of the higher homologues would stimulate subsequent experimental studies. In addition, the high stability of the anionic systems $X_{10}M^-$ is also of interest for future investigations.

■ COMPUTATIONAL METHODS

Quantum chemical computations are carried out using the Gaussian 03[21] and Molpro 06[22] suites of programs. Geometries and harmonic vibrational frequencies of the low-lying isomers are determined using density functional theory (DFT) method with the hybrid B3LYP functional, which involves the Becke three-parameter exchange[23] and Lee—Yang—Parr correlation[24] functionals. The initial search for all possible low-lying isomers of each of the clusters $X_{10}M^{0/-}$ considered is performed using a stochastic search algorithm, which was implemented by us,[25] on the basis of the Saunder's procedure.[16] First, the possible structures of the cluster $X_{10}M$ are generated by random "kick" method, and then rapidly optimized at the B3LYP/CEP-31G level.[26] In this "kick" procedure, the minimum and maximum distances between atoms are limited to 2 and 7 Å, respectively. Geometries of the stationary points located are then reoptimized using the B3LYP functional in conjunction with the LanL2DZ basis set, in which ab initio effective core potentials (ECPs) have been generated to replace the Coulomb, exchange and core-orthogonality effects of the chemically inert core electrons in transition metals.[27]

To obtain more accurate energetic predictions, calculations of single-point electronic energies of the global minima are further

9994

dx.doi.org/10.1021/jp111324n |J. Phys. Chem. A 2011, 115, 9993–9999
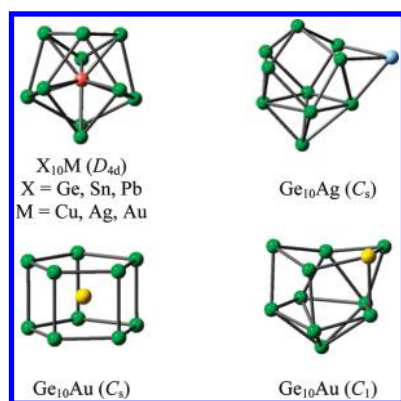
Figure 2. Shapes and point groups of some low-lying isomers of the neutral clusters $X_{10}M$ (X = Ge, Sn, Pb and M = Cu, Ag, Au) (B3LYP/LanL2DZ level).

performed using the coupled-cluster theory CCSD(T) method,[28] making use of the correlation consistent aug-cc-pVTZ-PP basis set, in which PP stands for relativistic pseudopotentials for metal atoms.[29] Densities of states are computed using the Pymolyze program.[30] The electron localizability indicator (ELI-D) values are calculated by using DGrid-4.2 program suite,[31] and the ELI isosurfaces are plotted using the Gopenmol software.[32]

■ RESULTS AND DISCUSSION

Geometries of Lower-Lying Isomers. The structures given hereafter are labeled by XY.n for the anions, where X = I, II, III stands for Ge, Sn, Pb and Y = A, B, C stands for Cu, Ag and Au, respectively. While the shapes, point groups, electronic states, and relative energies of the lower-lying isomers $X_{10}M^-$ are shown in Figure 1, the structures of the global minima $X_{10}M$ are given in Figure 2. The global minima of all copper doped group IVA clusters at the anionic state $X_{10}Cu^-$ (X = Ge, Sn, Pb) have high symmetry structure (D_{4d}, Figure 1a). It is interesting to see that the same structures D_{4d} are found to be the global minima for neutrals $X_{10}Cu$ (Figure 2). At the B3LYP/LanL2DZ level, the Ge−Cu bond length of the neutral $Ge_{10}Cu$ is equal to 2.55 Å, which represents the shortest distance as compared to those of Sn−Cu (2.80 Å) and Pb−Cu (2.86 Å). Following attachment of one excess electron, the distances of X−Cu of the anion $X_{10}Cu^-$ are slightly shortened (d(Ge−Cu) = 2.52 Å, d(Sn−Cu) = 2.75 Å, and d(Pb−Cu) = 2.82 Å), due to the closed shell electronic configuration of the anionic systems.

Following replacement of Cu by heavier impurities Ag and Au, the D_{4d} structure becomes unfavorable for doped Ge clusters. The C_2 structure IB.1 (Figure 1b) in which the Ag atom is doped outside of the Ge_{10} cage is found to be the global minimum for $Ge_{10}Ag^-$ with 16.5 kcal/mol lower in energy as compared to the D_{4d} structure IB.6. The structures IB.2 and IB.3 are the next isomers with relative energies of 6.0 and 8.2 kcal/mol, respectively. At the neutral state, a C_s structure (Figure 2), which is a lower symmetry of IB.1, is the global minimum for the neutral $Ge_{10}Ag$, while the D_{4d} structure is the next isomer with 10.7 kcal/mol higher in energy.

For $Ge_{10}Au^-$ anionic clusters (Figure 1c), two structures, including a D_{5h} structure IC.1 in which Au is located at center of a D_{5h} cage, and a C_1 structure IC.2 in which one Ge atom of the Ge_{11} is replaced by one Au atom are almost degenerate in energy. The next isomer is a D_{4d} structure IC.3 that is 12.2 kcal/mol less

stable than the first one. Following detachment of one electron, a C_s structure (Figure 2) that is distorted from a high symmetry IB.1 (D_{5h}) under a Jahn−Teller effect, is found to be the most stable isomer for the neutral $Ge_{10}Au$. Two structures, including a C_1 structure and a D_{4d} structure (Figure 2) are also quite stable with relative energies of 2.7 and 5.2 kcal/mol, respectively.

Let us note that the size of D_{4d} cages is smaller compared to that of D_{5h} counterparts. At the B3LYP/LanL2DZ level, the Au−Ge bond length of IC.1 (D_{5h}) is equal to 2.72 Å and that is larger than that of 2.64 Å of IC.3 (D_{4d}). This difference is not quite large but may be reason for why gold can be located at the center of the D_{5h} cage, while similar structures of silver dopant, which has a smaller atom radius, are not stable. Moreover, even for the gold doped germanium clusters $Ge_{10}Au^{0/-}$, there is a competition between the endohedral IC.1 and exohedral IC.2 structures. Their difference in relative energies is quite small for the neutrals $Ge_{10}Au$, and nearly zero for the anions $Ge_{10}Au^-$. These clusters are less stable as compared to other endohedral forms shown in the following sections.

Due to the larger size of the Sn_{10} and Pb_{10} cages, as compared to the Ge_{10} cage, it is expected that Ag and Au impurities can be encapsulated to form compact structures. Our calculations point out that all clusters $X_{10}M^{0/-}$ with X = Sn, Pb and M = Ag, Au are bicapped square antiprism structures (D_{4d}) (Figures 1 and 2). The X−M bonding lengths are slightly increased when moving down from Cu to Au as shown in Table 1.

Binding and Adiabatic-Vertical Detachment Energies. To probe the inherent stability of the anionic clusters considered, the average binding energies (BEs), vertical (VDE), and adiabatic (ADE) detachment energies of the lowest-lying $X_{10}M^{0/-}$ isomers are evaluated and compared to those of the pure dianionic clusters X_{10}^{2-} (D_{4d}). The average binding energies (BE) can be defined as follows:

$$BE = [nE(X) + E(M) - E(X_{10}M)]/(n+1) \quad for X_{10}M \tag{1}$$

$$BE = [nE(X) + E(M^-) - E(X_{10}M^-)]/(n+1) \quad for X_{10}M^- \tag{2}$$

$$BE = [(n-2)E(X) + 2E(X^-) - E(X_{10}^{2-})]/n \quad for X_{10}^{2-} \tag{3}$$

where $E(X)$, $E(M)$, $E(X^-)$, and $E(M^-)$ with X = Ge, Sn, Pb and M = Cu, Ag, Au are the total energies of the atoms at the neutral and anionic states, respectively.

While the BE, ADE, and VDE values of the lowest-lying isomers are given in Table 1, the plots of the BE values are illustrated in Figure 3a. Compared to the $X_{10}M$ systems containing 42 valence electrons reported earlier, namely BE($Ge_{10}Zn$) = 3.1 eV, BE($Sn_{10}Zn$) = 2.8 eV,[13] BE($Pb_{10}Mg$) = 1.77 eV, and BE($Pb_{10}Ba$) = 1.83 eV,[14] the isoelectronic species $X_{10}M^-$ are thus characterized by large BE values that ultimately indicate their higher stability. Although the neutrals $X_{10}M$ have somewhat lower stability than the corresponding anions due to their opened electronic shell, they also possess relatively high BE values. Additionally, it can be seen from Figure 3a that the doping by coinage metals (Cu, Ag and Au) results in increasing binding energies of the impure clusters $X_{10}M$ as compared to those of the pure X_{10}^{2-}.

9995

dx.doi.org/10.1021/jp111324n |*J. Phys. Chem. A* 2011, 115, 9993–9999

Table 1. Selected Geometrical Parameters, HOMO−LUMO Gaps (HLG) (eV), Vertical (VDE) and Adiabatic (ADE) Detachment Energies (eV), Embedding Energy (EE) (eV), and Average Binding Energy (BE) (eV) of the Global Minima $X_{10}M^{0/-}$ and X_{10}^{2-}

structure	d_{X-M} (Å)[a]	VDE[b]	ADE	BE	EE	HLG[c]
$Ge_{10}Cu$ (D_{4d}, $^2A_1$)	2.552; 2.662	6.47		2.98	3.18	
$Ge_{10}Ag$ (C_s, $^2A'$)	2.830	6.36		2.78	1.02	
$Ge_{10}Au$ (C_s, $^2A''$)	2.720	6.76		2.82	1.46	
$Sn_{10}Cu$ (D_{4d}, $^2A_1$)	2.795; 2.977	6.14		2.68	3.76	
$Sn_{10}Ag$ (D_{4d}, $^2A_1$)	2.880; 3.015	6.03		2.54	2.20	
$Sn_{10}Au$ (D_{4d}, $^2A_1$)	2.883; 3.019	5.93		2.65	3.33	
$Pb_{10}Cu$ (D_{4d}, $^2A_1$)	2.864; 3.093	5.93		2.43	3.56	
$Pb_{10}Ag$ (D_{4d}, $^2A_1$)	2.931; 3.117	5.84		2.33	2.47	
$Pb_{10}Au$ (D_{4d}, $^2A_1$)	2.948; 3.131	5.72		2.43	3.53	
$Ge_{10}Cu^-$ (D_{4d}, $^1A_1$)	2.520; 2.849	3.06	2.79	3.15	5.10	2.48
$Ge_{10}Ag^-$ (C_2, ^1A)	2.711	3.31	3.05	2.97	2.52	2.21
$Ge_{10}Au^-$ (D_{5h}, $^1A'_1$)	2.721	3.17	3.02	2.92	3.08	2.19
$Sn_{10}Cu^-$ (D_{4d}, $^1A_1$)	2.753; 3.204	3.11	2.91	2.87	5.80	2.39
$Sn_{10}Ag^-$ (D_{4d}, $^1A_1$)	2.845; 3.218	2.99	2.79	2.71	4.01	2.16
$Sn_{10}Au^-$ (D_{4d}, $^1A_1$)	2.848; 3.236	2.90	2.68	2.71	4.06	2.07
$Pb_{10}Cu^-$ (D_{4d}, $^1A_1$)	2.819; 3.314	2.97	2.84	2.61	5.53	2.58
$Pb_{10}Ag^-$ (D_{4d}, $^1A_1$)	2.892; 3.320	2.85	2.71	2.49	4.19	2.39
$Pb_{10}Au^-$ (D_{4d}, $^1A_1$)	2.908; 3.346	2.75	2.59	2.49	4.17	2.26
Ge_{10}^{2-} (D_{4d}, $^1A_1$)				2.92		2.86
Sn_{10}^{2-} (D_{4d}, $^1A_1$)				2.55		2.39
Pb_{10}^{2-} (D_{4d}, $^1A_1$)				1.97		0.51

[a] The first value is bond length between metal (M) and X atoms of cage X_8. The second value is bond length between metal (M) and X atoms in the C_4 axis. [b] Values of VDE, ADE, EE, and BE calculated at the CCSD(T)/aug-cc-pVTZ-PP level. [c] HOMO−LUMO gaps are obtained at the B3LYP/LanL2DZ level.

Let us stress that the average binding energy (BE) is only one of the energetic properties used to evaluate the stability of clusters. It can be seen that the difference in BEs between $Ge_{10}X$ (X = Ag, Au) and $Ge_{10}Cu$ is relatively larger than those of the corresponding $Sn_{10}X$ or $Pb_{10}X$ clusters. For the neutral state, the difference in BEs between $Ge_{10}Cu$ and $Ge_{10}Au$ is 0.16 eV (0.2 eV for $Ge_{10}Ag$). This difference between $Sn_{10}Cu$ and $Sn_{10}Au$ amounts to only 0.03 eV (0.14 eV for $Sn_{10}Ag$), whereas the BE of $Pb_{10}Cu$ and $Pb_{10}Au$ is nearly the same. This indicates a lower stability of the opened structure $Ge_{10}Ag$ as compared to the packing structure $Ge_{10}Cu$. The lower stability of $Ge_{10}Au$ can be understood from the larger size of the D_{5h} cage. Similar observations can be found for the anionic clusters. For the VDE and ADE values, it can be observed that the presence of dopants forms similar trends in both the neutral and anionic states. The VDE (and ADE for anionic clusters) values are remarkably high, and only slightly decrease when moving down from Cu to Au.

Embedding Energy (EE). Embedding energy is the energy gain in incorporating a dopant M = Cu, Ag, and Au into a X_{10} cage (X = Ge, Sn, Pb) and defined as follows:

$$EE(X_{10}M) = E(X_{10}) + E(M) - E(X_{10}M) \qquad \textit{for a neutral } X_{10}M$$

$$EE(X_{10}M^-) = E(X_{10}) + E(M^-) - E(X_{10}M^-) \qquad \textit{for an anion } X_{10}M^-$$
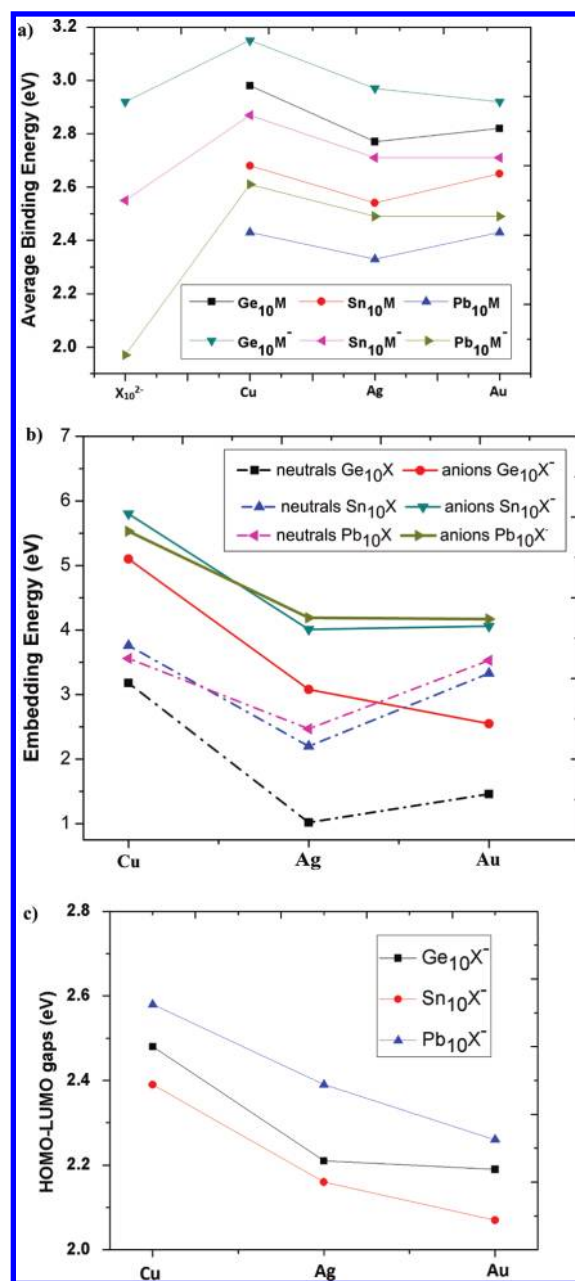

Figure 3. Plots of (a) binding energies (eV), (b) embedding energies (eV) and (c) HOMO-LUMO gaps of the global minima $X_{10}M^{0/-}$ and X_{10}^{2-}.

where $E(X_{10})$ is the total energy of the global minima X_{10} (C_{3v}).[25]

Embedding energy can thus be used for evaluating the stability of endohedrally doped structures. The EE values of the global minima $X_{10}M$ at both neutral and cationic states are given in Table 1, while the relevant plots are depicted in Figure 3b. At the first glance, there exists a similar trend between the binding energy and embedding energy values. The EE values of the anions $X_{10}M^-$ with closed electronic shells are considerably larger than those of the open shell neutrals $X_{10}M$. The embedding energies of endohedral structures $Ge_{10}Cu^{0/-}$ are found to be remarkably large as compared to those of exohedral structures $Ge_{10}Ag^{0/-}$. In addition, the EE values of the clusters $Ge_{10}Au^{0/-}$
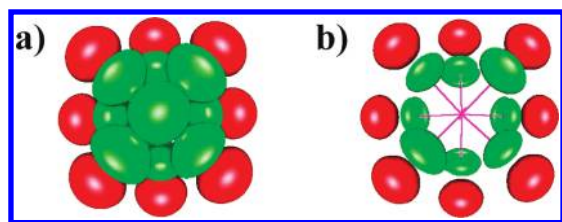
9996

dx.doi.org/10.1021/jp111324n |*J. Phys. Chem. A* 2011, 115, 9993–9999

Figure 4. Densities of states of the global minimum $Ge_{10}Cu^-$ (D_{4d}).

are small with respect to those of the clusters $Ge_{10}Cu^{0/+}$. It seems that the endohedral forms (D_{5h}) of $Ge_{10}Au$ clusters are less stable due to the large size of the D_{5h} cages. This result is consistent with the previous finding that $Ge_{10}Au$ is not an species with enhanced stability in the series of small gold doped germanium clusters Ge_nAu.[19] Our EE values also show that endohedral structures D_{4d} exhibit remarkably larger values than those of exohedral and D_{5h} structures.

HOMO−LUMO Gaps. The frontier orbital energy gaps (HLG) can be considered as a measure of kinetic stability of chemical compounds. A large HLG gap suggests a high reluctance of compounds for chemical reactions. The HLG values of the closed shell systems $X_{10}M^-$ are given in Table 1, their plots are displayed in Figure 3c. Similar to the case of VDE and ADE values, Cu-doped anionic clusters reveal the highest HLG values, which somewhat decrease in going to Ag and Au. All anionic systems bear high energy gaps as compared to those of systems previously reported (HLG (eV) = 2.0 for Be@Ge$_{10}$, 1.9 for Be@Sn$_{10}$, 1.9 for Ge$_{10}$Zn, and 1.6 for Zn@Sn$_{10}$),[13] which lend a further support for their enhanced stabilities. It is especial to note the energy gaps of the doped Pb clusters $Pb_{10}M^-$ (HLG = 2.26−2.58 eV) are improved substantially in comparison to their host Pb_{10}^{2-} (HLG = 0.51 eV)

Electronic Structure and Chemical Bonding. As for a prototypical case, an analysis of the MOs and their densities of state (DOS) of the anion $Ge_{10}Cu^-$ are performed. While the plots of total and partial densities of state (pDOS) for $Ge_{10}Cu^-$ are shown in Figure 4, the plots of total DOS for all global minima $X_{10}M^-$ and pure clusters X_{10}^{2-} are given in Figure 5.

MOs shape and their energy levels displayed in Figure 4 indicate that the 42 valence electrons of $Ge_{10}Cu^-$ (D_{4d}) are distributed in the following electron configuration: $[1a_1^2 1b_2^2 1e_1^4 2a_1^2 1e_2^4 1e_3^4 3a_1^2 4a_1^2 2e_2^4 2e_3^4 2b_2^2 3e_2^4 2e_1^4 5a_1^2]$. This corresponds to the following energy sequence of electronic shell model $[1S^2 1P^6 1D^{10} 1F^2 2S^2 1F^8 2P^2 1F^4 2P^4 1G^2]$. The lowest MO is an s-type valence orbital, being followed by three p-type orbitals of the $1P^6$ subshell. Due to a lowering symmetry of $Ge_{10}Cu^-$ (D_{4d}), the f-type valence orbitals are splitting into 2P subshell and the nonbonding d-orbitals of copper. While orbitals of 1S and 1P subshells are mainly composed of s-AO(Ge), an interaction between s-AO(Ge) and d-AO(Cu) is found for the 1D-orbitals. The DOS plots also reveal that s-orbital of the 2S subshell is a symmetric combination of 4s-AO and 4p-AOs of Ge

Figure 5. Plots of total densities of states (DOS) of the global minima $X_{10}M^-$ and X_{10}^{2-} (X = Ge, Sn, Pb and M = Cu, Ag, Au).

and 4s-AO of Cu, whereas the presence of 4p-AOs of Cu actually stabilizes the 2P subshell. It is remarkable that while the LUMOs are only composed of p-AO(Ge), an important contribution of s-AO(Ge) and d-AO(Cu) is found in the HOMO. As a

Figure 6. Isosurfaces of p-ELI plots for Ge10Cu⁻ at ELI values of (a) 0.6 and (b) 0.8.

consequence, a large energy gap between frontier orbitals emerges leading to a high stability of $Ge_{10}Cu^-$.

The plots of total DOS of the global minima $X_{10}M^-$ (Figure 5) show that addition of a coinage metal dopant lowers the energy levels of the mixed clusters, relative to the pure X_{10}^{2-} dianionic cages. The shifting of energy levels of $X_{10}M^-$ consistently increases in going from Cu to Au as dopant.

Electron Localization. An inspection of the electron localizability indicator (ELI),[33] which is proved to be an effective tool to probe the chemical bonding in organic compounds as well as in transition metal compounds,[34,35] is performed. Let us show an analysis of the ELI of $Ge_{10}Cu^-$. The isosurfaces of partial-ELI distribution for this anion given in Figure 6 reveal that the green localization domains arising from σ-orbitals are distributed between Ge atoms. Consequently, they are responsible for bonding between Ge atoms of the cages. The red domains composed of π-orbitals are distributed globally over Ge atoms of the cage and is expected to be responsible for π-aromaticity.

Three-Dimensional Aromaticity. Aromaticity is well recognized as a measure of stability of chemical compounds. While aromaticity of planar structures can be qualitatively probed by using Hückel rule of $(4n + 2)$ valence electrons,[36] the $2(N + 1)^2$ electron count rule, which is recently proposed by Hirsch et al.,[37] is proven to be an effective criterion for spherical structures. In the latter counting framework, the π-electron system of fullerenes can approximately be considered as a spherical electron gas which surrounds the surface of a sphere (I_h). The wave functions of this electron gas can be characterized by the angular momentum quantum numbers ($l = 0, 1, 2, 3, ...$) that are comparable to the atomic s, p, d, f, ... orbitals. According to the classical Pauli principle, if a spherical system bearing $2(N + 1)^2$ π-electrons fully fills all π-shells, it then is stabilized and exhibits an aromatic character.

Let us now consider the MO pictures of the global minimum $Ge_{10}Cu^-$ shown in Figure 4. The valence orbitals of $Ge_{10}Cu^-$ can be divided into two subsets, the first contains the MOs of the shells $1S(A_1, \sigma)$, $1P(B_2, \sigma)$ $1P(E_1, \sigma)$, $1D(A_1, \sigma)$ $1D(E_2, \sigma)$ $1D(E_3, \sigma)$ and $1F(A_1, \sigma)$ $1F(E_2, \sigma)$ $1F(E_3, \sigma)$ $1F(E_2, \sigma)$ and $1G(A_1, \sigma)$ that are occupied by 34 σ-electrons. The second subset includes the MOs of the shells $2S(A_1, \pi)$, $2P(B_2, \pi)$, and $2P(E_1, \pi)$, which are occupied by 8 valence π-electrons. As a consequence, this π-electron system makes $Ge_{10}Cu^-$ three-dimensionally π-aromatic satisfying the $2(N + 1)^2$ count rule. Similar systems of 8 valence π-electrons are also found as the global minima of the clusters $X_{10}M^-$, including $Sn_{10}Cu^-$, $Sn_{10}Ag^-$, $Sn_{10}Au^-$, $Pb_{10}Cu^-$, $Pb_{10}Ag^-$, and $Pb_{10}Au^-$, and accordingly, they also have a spherical π-aromatic character.

■ CONCLUDING REMARKS

In the present theoretical study, we perform a systematic investigation on the coinage metal encapsulated group 14 clusters $X_{10}M^{0/-}$ at the neutral and anionic states, including X = Ge, Sn, Pb and M = Cu, Ag, Au. The global minima are located using a stochastic search method. Except for the $Ge_{10}Ag$, the global minima of most $X_{10}M^{0/-}$ systems considered are endohedral structure with impurities encapsulated at the center of X_{10} cages. The calculated results reveal a high stability of systems having large frontier orbital energy gaps, high vertical and adiabatic detachment energies, large embedding and binding energies. These predictions are in good agreement with available experimental results for enhanced stability of the $X_{10}Cu$ clusters with X = Sn and Pb. Electronic structure and chemical bonding of the global minima are also considered using density of states (DOS) of molecular orbitals, and topology analysis of the electron localizability indicator (ELI). The global minima with D_{4d} structure turn out to be magic clusters that can be rationalized in terms of their high spherical aromaticity. We would hope that appropriate experimental studies probing these enhanced stability systems could be carried out in a near future.

■ ASSOCIATED CONTENT

ⓢ Supporting Information. Shapes and relative energies of low-lying isomers of $X_{10}Cu^-$, $X_{10}Ag^-$, and $X_{10}Au^-$. Total density of states plots of global minima of $X_{10}M^-$ and X_{10}^{2-}. This material is available free of charge via the Internet at http://pubs.acs.org.

■ AUTHOR INFORMATION

Corresponding Author
*E-mail: minh.nguyen@chem.kuleuven.be.

■ ACKNOWLEDGMENT

■ REFERENCES

(1) Chen, X.; Deng, K.; Liu, Y.; Tang, C.; Yuan, Y.; Tan, W.; Wang, X. *J. Chem. Phys.* **2008**, *129*, 094301.

(2) Schafer, S.; Schafer, R. *ChemPhysChem* **2008**, *9*, 1925.

(3) Spiekermann, A.; Hoffmann, S. D.; Fassler, T. F. *Angew. Chem., Int. Ed.* **2006**, *45*, 3459.

(4) Scharfe, S.; Fassler, T. F.; Stegmaier, S.; Hoffmann, S. D.; Ruhland, K. *Chem.—Eur. J.* **2008**, *14*, 4479.

(5) Kumar, V.; Kawazoe, Y. *Appl. Phys. Lett.* **2003**, *83*, 2677.

(6) Matxain, J. M.; Piris, M.; Formoso, E.; Mercero, J. M.; Lopez, X.; Ugalde, J. M. *ChemPhysChem* **2007**, *8*, 2096.

(7) Cui, L. F.; Huang, X.; Wang, L. M.; Li, J.; Wang, L. S. *Angew. Chem., Int. Ed.* **2007**, *46*, 742.

(8) Lu, J.; Nagase, S. *Chem. Phys. Lett.* **2003**, *372*, 394.

(9) Li, G.; Zhang, X.; Tang, Z.; Gao, Z. *Chem. Phys. Lett.* **2002**, *359*, 203.

(10) Xing, X.; Tian, Z.; Liu, H.; Tang, Z. *Rapid. Commun. Mass. Spectrom.* **2003**, *17*, 1411.

(11) (a) Tai, T. B.; Nguyen, M. T. *Chem. Phys. Lett.* **2010**, *492*, 290. (b) Tai, T. B.; Nguyen, H. M. T.; Nguyen, M. T. *Chem. Phys. Lett.* **2011**, *502*, 187.

(12) Chen, Z.; Neukermans, S.; Wang, X.; Janssens, E.; Zhou, Z.; Silverans, R. E.; King, R. B.; Schleyer, P. v. R.; Lievens, P. *J. Am. Chem. Soc.* **2006**, *128*, 12829.

(13) Kumar, V.; Singh, A. K.; Kawazoe, Y. *Nano Lett.* **2004**, *4*, 677.

(14) Rajesh, C.; Majumder, C. *J. Chem. Phys.* **2008**, *128*, 024308.

(15) (a) Ngan, V. T.; Grune, P.; Claes, P.; Janssens, E.; Fielicke, A.; Nguyen, M. T.; Lievens, P. *J. Am. Chen. Soc.* **2010**, *132*, 15589. (b) Veldeman, N.; Gruene, P.; Fielicke, A.; Claes, P.; Ngan, V. T.; Nguyen, M. T.; Lievens, P. Endohedrally Doped Silicon Clusters. In *Handbook of Nanophysics. Clusters and Fullerenes*; Sattler, Klaus D., Ed.; CRC Press: Boca Raton, FL, 2010; Chapter 5.

(16) (a) Gopakumar, G.; Wang, X.; Lin, L.; De Haeck, J.; Lievens, P.; Nguyen, M. T. *J. Phys. Chem. C* **2009**, *113*, 10858. (b) Hou, X. J.; Gopakumar, G.; Lievens, P.; Nguyen, M. T. *J. Phys. Chem. A* **2007**, *111*, 13544.

(17) Neukermans, S.; Wang, X.; Veldeman, N.; Janssens, E.; Silverans, R. E.; Lievens, P. *Int. J. Mass. Spectrom.* **2006**, *252*, 145.

(18) Wang, J.; Han, J. G. *J. Chem. Phys.* **2005**, *123*, 244303.

(19) Li, X. J.; Su, K. H. *Theor. Chem. Acc.* **2009**, *124*, 345.

(20) Saunders, M. *J. Comput. Chem.* **2003**, *25*, 621.

(21) Frisch, M. J.; et al. *Gaussian 03*, Revision D.02; Gaussian, Inc.: Wallingford, CT, 2004.

(22) Werner, H. J.; et al. *Molpro*, a package of ab initio programs, version 2008.1.

(23) Becke, A. D. *J. Chem. Phys.* **1993**, *98*, 5648.

(24) Lee, C.; Yang, W.; Parr, R. G. *Phys. Rev. B.* **1988**, *37*, 785.

(25) Tai, T. B.; Nguyen, M. T. *J. Chem. Theor. Comput.* **2011**, *7*, 1119.

(26) Stevens, W. J.; Krauss, M.; Basch, H.; Jasien, P. R. *Can. J. Chem.* **1992**, *70*, 612.

(27) Hay, P. J.; Wadt, W. R. *J. Chem. Phys.* **1985**, *82*, 270.

(28) Bartlett, R. J.; Musial, M. *Rev. Mod. Phys.* **2007**, *79*, 291 and references therein.

(29) Peterson, K. A. *J. Chem. Phys.* **2003**, *119*, 11099.

(30) Tenderholt, A. *Pymolyze: a program to analyze quantum chemical computations*. 2006

(31) Kohout, M. *DGrid-4.2*; Max-Planck Institut fur Chemische Physik und Fester Stoffe: Dresden, 2007.

(32) Laaksonen, L. *J. Mol. Graph.* **1992**, *10*, 33.

(33) Wagner, F. R.; Bezuly, V.; Kohout, M.; Grin, Y. *Chem.—Eur. J.* **2007**, *13*, 5724.

(34) Kohout, M.; Wagner, F. R.; Grin, Y. *Theor. Chem. Acc.* **2002**, *108*, 150.

(35) (a) Tai, T. B.; Nguyen, M. T. *Chem. Phys. Lett.* **2010**, *489*, 75. (b) Ngan, V. T.; Nguyen, M. T. *J. Phys. Chem. A* **2010**, *114*, 7609. (c) Holtzl, T.; Veldeman, N.; De Haeck, J.; Veszpremi, T.; Lievens, P.; Nguyen, M. T. *Chem.—Eur. J.* **2009**, *15*, 3970. (d) Lin, L.; Holtzl, T.; Gruene, P.; Claes, P.; Meijer, G.; Fielicke, A.; Lievens, P.; Nguyen, M. T. *ChemPhysChem* **2008**, *9*, 2471.

(36) Boldyrev, A. I.; Wang, L. S. *Chem. Rev.* **2005**, *105*, 3716.

(37) Hirsch, A.; Chen, Z.; Jiao, H. *Angew. Chem., Int. Ed.* **2000**, *39*, 3915.